

A two-stage hair region localization method for guided laser hair removal

Murat AVŞAR[✉], İmam Şamil YETİK^{*}

Department of Electrical and Computer Engineering, Faculty of Engineering,
TOBB University of Economics and Technology, Ankara, Turkey

Received: 20.09.2019

Accepted/Published Online: 14.05.2020

Final Version: 27.01.2021

Abstract: Removal of hair using laser is a widely used method, where our goal is to permanently remove hair by using laser to cause heat in order to thermally damage the hair follicle. However, currently available laser hair removal systems affect the outer skin layers besides hair follicles. This is a disadvantage of classical methods with major health risks. We propose a method to overcome these health risks by guiding the laser beam only to automatically localized hair regions. This study aims to develop an automated feature-based hair region localization method as an integral part of the proposed hair removal system utilizing laser, a first attempt in this area. The quantitative analysis and visual evaluation of the results obtained with the proposed technique shows that it is possible to automatically localize hair regions for guided laser hair removal. We believe this study, a first in this area, will open the way to researchers interested to attack this problem.

Key words: Automated hair localization, guided laser epilation, image processing

1. Introduction

Classical hair removal methods have a short term effect resulting in hairs to grow again. Therefore permanent laser hair removal approaches have received significant attention, e.g., [1, 2]. Classical methods of permanent hair removal systems are performed with a laser beam blindly affecting all areas of the skin regardless of the fact that a particular area has hair or not. Certain pigments called chromophores absorb the laser, causing the hair roots to be damaged [3–5]. Laser directed to a hair root causes heat on the hair root thereby permanently damaging it preventing future hair growth. This process is called “selective photothermolysis theory” [6]. Most hair removal systems using laser target melanin, the main hair chromophore, by converting radiation to heat and thereby permanently damaging the hair root. Red and near infrared frequencies are used to achieve this damaging capability. Despite many techniques embedded in laser hair removal systems to prevent overheating the skin, undesired health risks unfortunately still occur [3–5, 7]. In this paper, we develop a guided laser removal procedure to avoid these significant health risks by using laser on automatically localized hair roots with computer vision techniques.

2. Smart laser epilation with computer aided techniques

There are approaches to minimize these risks including using a laser beam with a smaller radius. However, these devices using small spot size laser are not commonly used because of the need for more skilled and experienced operators. To overcome these problems, we develop a new technique where we automatically locate hair regions

*Correspondence: syetik@etu.edu.tr

using image processing techniques and feed these locations to laser for guided epilation. Our proposed technique is a first in this area. The schema of the proposed laser hair removal technique is illustrated in Figure 1. In this model, hair regions are being localized by image processing unit utilizing methods we have developed in this paper. Based on the outputs of the image processing unit (automatically localized hair roots), small spot sized laser beam is moved over the detected hair regions only.

In this paper, we develop a novel two-stage method to automatically localize hair roots using image processing and supervised feature-based techniques. Then these locations are fed to a small spot-sized laser device. In this way, we are able to damage only the hair roots rather than the whole skin area. Feature vectors are developed to distinguish between hair and nonhair regions. Scale, rotation, illumination, skin and hair color invariance is aimed with the selected features, where the differentiation power between these classes can be preserved. Performance of the proposed classifier is tested using sensitivity and specificity values of the method and by measuring the processing time of the classifier.

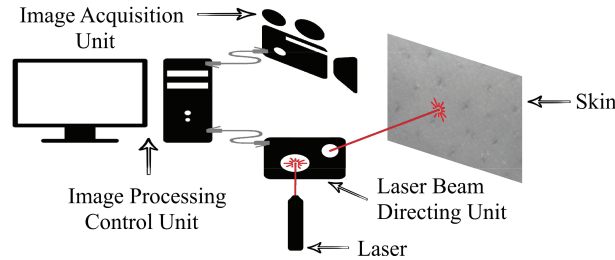


Figure 1. Proposed small spot-sized computer-assisted laser hair removal system. Figure shows several components and their role in the system.

3. Related work

Detection of hair regions automatically are studied for other problems such as skin lesions previously. These methods uses a different approach entirely and has not been utilized to construct a laser epilation system that is able to target hair roots only. Therefore, our efforts pave the way to a new research area of guided laser epilation. Hairs present on a skin results in deteriorated performance for lesion detection. In order to overcome this problem, hairs are first localized and removed as a prior preprocessing step. Abbas et al. and other studies [8, 9] proposed a localization method utilizing a Gaussian filter to detect the hairs in the image coarsely. More precised locations of the hairs are obtained with a line joining algorithm. Fiorese et al. [11] used adaptive median filtering prior to segmentation for improved performance through the method developed in [10], and developed a hair localization method where candidate areas are found with a top-hat operator, then a decision tree is used for fine tuning. Another study uses matched filters for hair detection [12]. A set of filters consisting of eighteen filters are convolved with the image and the one with the highest response is selected as the value for that pixel.

None of these techniques utilize machine learning approaches, and thus all of them are prone to disadvantages of absence of training data. In this paper, we develop a machine learning based hair localization method that utilizes training data. In our preliminary studies, we proposed a feature-based machine learning approach for hair region detection on skin images [13]. In these studies, only features with low computational complexity had been chosen for real-time applications. In this study we propose to use more advanced features with high computational complexity without causing a significant speed problem achieving improved performance. We also propose a new novel two-stage classification model and prove the effectiveness with extensive tests.

4. Methodology

4.1. System overview

In this paper, a two-stage feature-based classification system is being proposed as illustrated in Figure 2. In the first stage of this model, classification is performed using features with low computational complexity. In the second stage, features with high computational complexity are also included in the classification process for improved hair region detection performance over coarsely segmented hair regions. Main goal of the proposed two-stage classification model is to increase the classification speed while maintaining the high detection rates which can be achieved with single stage classification models using complicated features. In order to extract features, test performances of each feature and analyze classification models, Matlab programming environment had been used. In the feature extraction stage of the proposed model nonoverlapping square shaped windows with the size of 15×15 pixels, have been utilized for the extraction of the patterns. This system classifies each 15×15 pixel pattern as hair or skin regions.

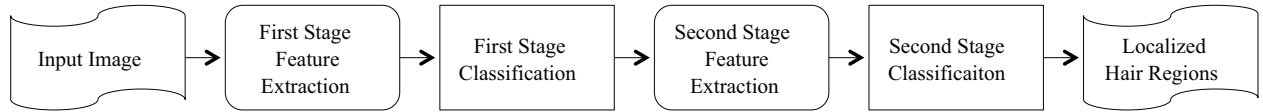


Figure 2. Two-stage classification scheme. First stage is faster eliminating obvious nonhair regions, while the slower second stage more accurately classifies hair regions processing fewer samples.

4.2. Image acquisition

In this study, a Point Grey Flea3 3.2 MP Mono camera with 25 mm fixed focal length compact lens has been used for image acquisition. Halogen light source is used for the illumination of the skin surface. Skin surface is flattened with help of a plate glass. Flattening of the skin surface provides uniform distribution of light over the surface. Images are taken from a fixed distance of about 10cm. Acquired 640×480 pixel images represent approximately 1.6 cm^2 skin region. Before the acquisition of the images, hairs are shaved to be about 1 mm in length. An image library, consisting of approximately 150 skin images, is constructed by using images taken from 10 participants who have Mediterranean skin type. Skin images are taken from legs, arms, and facial regions of the participants.

4.3. Construction of ground truth

Ground truth images are obtained by manually labeling regions as hair and nonhair on each image. A 15×15 pixel window size used in this study. Ground truth data obtained by manual labeling are being used for training and testing purposes while evaluating the performance of the classification models utilized in this study..

4.4. Features developed for classification

In this study, we developed features constructing a vector discriminating hair and nonhair regions using twelve different features. Scale, rotation and partially illumination invariances are achieved by carefully selecting appropriate features. Image preprocessing steps, such as image enhancement including contrast improvement are not being used, instead features are calculated from the raw image data such that possible information loss is prevented. These features are briefly explained below with their formulae, where R represents the neighboring region, N is the total number of pixels in this region, I is the average intensity level inside R , and $I(x, y)$ gives

the intensity value at pixel position (x, y) . Feature 1: Variance of intensities represents how far intensity values inside R spread out and it is calculated as

$$f_1 = \frac{1}{N} \sum_{x,y \in R} (I(x, y) - \mu_I)^2, \quad x, y \in R, \quad (1)$$

where x and y represents coordinates of each pixel inside gray level intensity image I . Feature 2: Intensity span (contrast) represents the difference between maximum and minimum intensity levels inside R and it is calculated as

$$f_2 = (\max(I(x, y)) - \min(I(x, y))) / \mu_I, \quad x, y \in R, \quad (2)$$

Feature 3: In this study outlier intensity levels are considered to be %5 higher or lower than the average intensity level inside R. Ratio of the bright intensity outliers count to overall pixel count is calculated as

$$f_3 = (\#(I(x, y) > 1.05 * \mu_I)) / N, \quad x, y \in R, \quad (3)$$

Feature 4: Ratio of the dark intensity outliers count to overall pixel count is calculated as

$$f_4 = (\#(I(x, y) < 0.95 * \mu_I)) / N, \quad x, y \in R, \quad (4)$$

Feature 5: Ratio of above mean pixel count to below mean pixel count is a measure of asymmetry for the histogram data of intensities inside R and it is calculated as

$$f_5 = (\#(I(x, y) < \mu_I)) / (\#(I(x, y) > \mu_I)), \quad x, y \in R, \quad (5)$$

Feature 6: Intensity mean and minimum intensity difference represents how far higher intensity levels spread out inside R and it is calculated as

$$f_6 = \mu_I - \min(I(x, y)), \quad x, y \in R, \quad (6)$$

Feature 7: Histogram peak of the region can also be called mode frequency of intensity levels inside R. Mode is the intensity level that occurs most often inside R. This feature is calculated as

$$f_7 = \frac{\max(\text{hist}_I(k)) \times \text{argmax}_k(\text{hist}_I(k))}{N \times \mu_I} \quad (7)$$

where $\text{hist}_I(k)$ is the histogram function for the pattern image.

Feature 8: Suppressed regional minima difference feature calculates the normalized difference between the original image and h-minima transform of that image. This feature is calculated as

$$f_8 = \frac{1}{N} \sum_R (\text{hminima}(I, th) - I(x, y)) \quad x, y \in R, \quad (8)$$

where $\text{hminima}(I, th)$ h-minima transform of the image and the threshold value th is defined as 35 which is determined by inspection of hair/skin discrimination results of this feature. H-minima transform suppresses all regional minima intensity levels on image I . In this study regional minimas are connected pixels with constant intensity level which is less than the intensity level of boundary pixels by at least value of th . In order to calculate the h-minima transform of the image, this study uses hybrid grayscale reconstruction algorithm which

is described by Vincent [14].

Feature 9: Entropy is a measure of randomness for the intensity levels inside R which is used in order to characterize the texture of the image. This feature is calculated as

$$f_9 = - \sum_{k=0}^{L-1} p_k \log_2(p_k), \quad L = 256, \quad (9)$$

where p_k is histogram counts for the pattern image.

Feature 10: Normalized third central moment is calculated by normalizing the third central moment of the image with variance of the image and it is calculated as

$$f_{10} = \frac{\frac{1}{N} \sum_R (I(x, y) - \mu_I)^3}{\sigma_I^2}, \quad x, y \in R, \quad (10)$$

where σ_I^2 is variance of the pattern image.

Feature 11: Interquartile range is the difference between upper and lower quartiles of the intensity image and it is calculated as

$$f_{11} = Q_3 - Q_1, \quad (11)$$

where Q_3 is the upper quartile intensity value and Q_1 is the lower quartile intensity value inside R.

Feature 12: Local minimum filter finds the minimum intensity level inside 3×3 pixel sliding window and replaces the central pixel value with the minimum intensity level. Local minimum filter difference feature calculates the normalized difference between original image and the filtered image. This feature is calculated as

$$f_{12} = \frac{1}{N} \sum_R (I(x, y) - I_{localMin}(x, y)) \quad x, y \in R, \quad (12)$$

where $I_{localMin}(x, y)$ is the local minimum filtering function. By using 8-connected neighborhoods of each pixel coordinate on image I, $I_{localMin}(x, y)$ is calculated as

$$I_{localMin}(x, y) = \min(I(x-1, y-1), I(x, y-1), I(x+1, y-1), I(-1, y), I(x, y), \quad (13)$$

$$I(x+1, y), I(x-1, y+1), I(x, y+1), I(x+1, y+1)); \quad x, y \in R. \quad (14)$$

Some of the example scatter plots of the features described above are shown in Figure 3 for the training data. The feature pairs shown in Figure 3 are best feature pairs where hair and skin data separations can be observed very clearly. Most effective features which have the best separation between hair and skin patterns are Features 4, 6 and 8. However, in this study, all features are examined together. We have utilized feature selection in order to find best combinations of all features. Due to the small number of features, this study uses an exhaustive feature selection method. Exhaustive feature selection technique implements the performance analysis for all of the possible subsets of 12 features and finds the optimal feature combination. Performance analysis for each feature subset is being performed by using 5-fold cross validation technique with 100 repetitions. Results from different repetitions are being averaged and the feature subset with minimum error rate is being selected as the optimal feature subset.

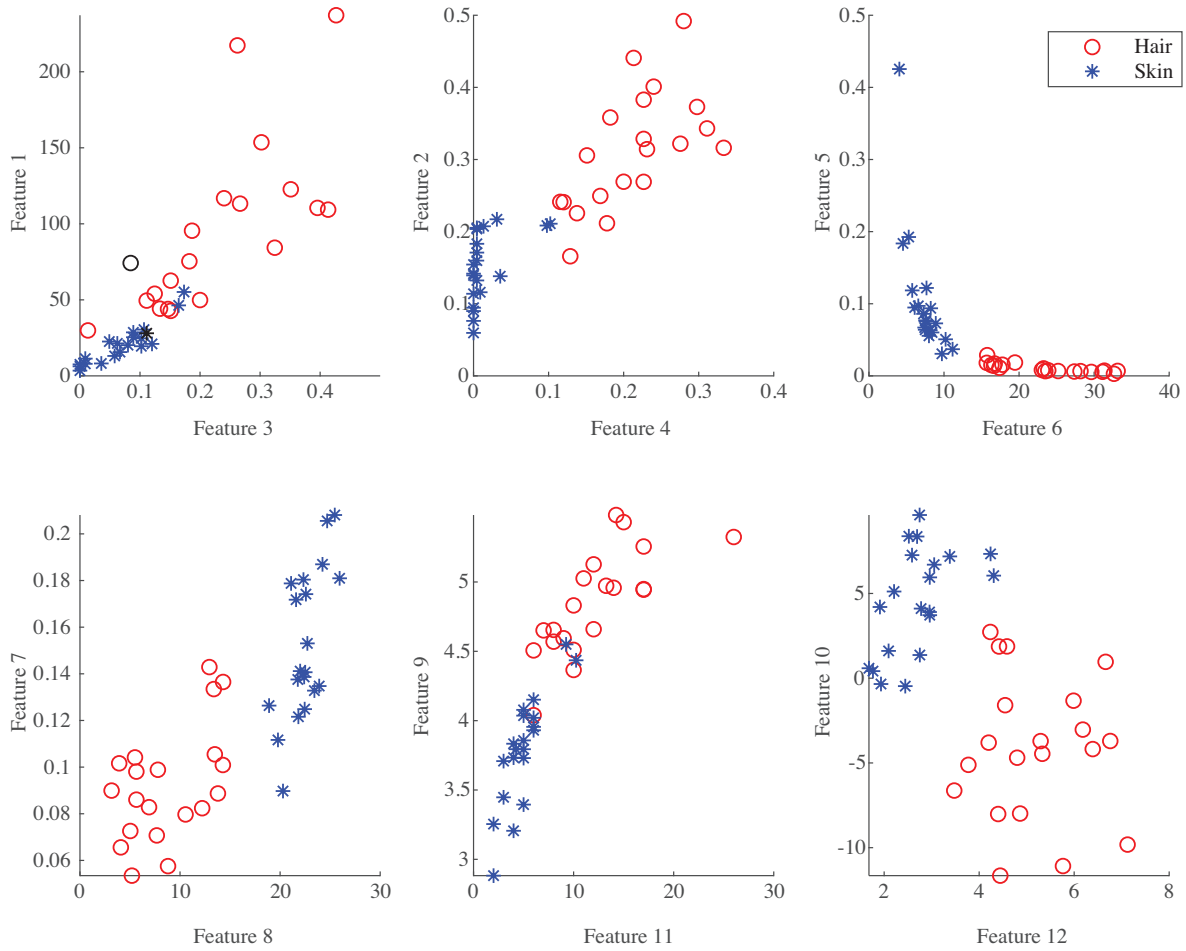


Figure 3. Distribution of features for our dataset. Figure shows how hair and nonhair regions are distinguishable with the proposed features.

5. Performance analysis

5.1. Setup

In this study, five different supervised classification techniques are utilized: linear discriminant analysis (LDA), support vector machines (SVM) with linear kernel, decision trees, naive Bayes, and k-nearest neighbor (K-NN) [9]. For each classification method, sensitivity, specificity, and error rate are being calculated. This study evaluates two stage cascaded classification model which examines feature sets with respect to their performances. The main idea of fast/slow feature separation and using slow features at the second stage of classification model is to increase the speed of hair detection process. This cascaded detection model is expected to increase the speed, however we also tried not to lose hair detection accuracy of this two-stage model with respect to single stage classification model. Therefore, performance of the proposed two-stage classification model is evaluated and compared to single-stage classification models that are using the same feature sets with first and second stage classifiers of the proposed model. These feature sets are selected prior to performance analysis. Results of the feature selection process are examined under two different titles: (i) Feature Set 1 (FS1); (ii) Feature Set 2 (FS2). As illustrated in Figure 4, feature set selected from fast features is called FS1 while feature set

selected from all twelve features is called FS2. By utilizing two different feature selection results over single-stage models, single-stage classification model 1 (SSCM1) and single-stage classification model 2 (SSCM2) are obtained, which are shown in Figures 5a and 5b. The classification speed of SSCM1 is expected to be higher than the speed of SSCM2, since SSCM1 uses only the fast features. On the other hand, classification success of SSCM2 is expected to be higher than the success of SSCM1, since SSCM2 uses more complex features too, which have high discrimination between hair and skin regions. Classification speed of the proposed system TSCM is expected to be higher than the speed of SSCM2 and lower than the speed of SSCM1. Hair region detection rate (sensitivity) of the TSCM shown in Figure 6 is expected to be lower than both of the single-stage models, since misclassified hair regions at the first stage, are not reclassified in the second stage of the TSCM. Sensitivity of the proposed TSCM can be higher than sensitivity of SSCM1 and close to sensitivity of SSCM2 only if the first stage sensitivity of TSCM is higher than the sensitivity of SSCM1. In this study, in order to boost the sensitivity of the first stage classifier, a biased cost function is used while training of first stage classifier. At the training stage of first stage classifier, prior probabilities of hair and skin classes are updated with respect to the misclassification costs described in the cost matrix.

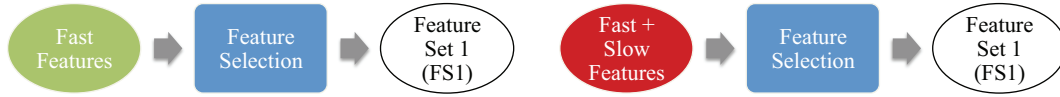


Figure 4. Feature Set 1 (first stage features) including fast features, Feature Set 2 (second stage features) including all features.

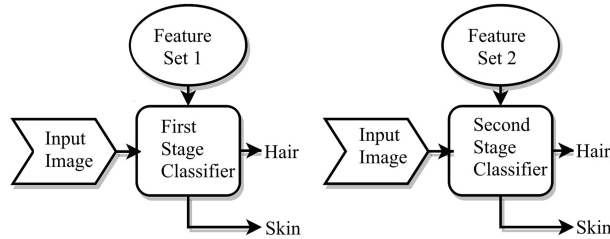


Figure 5. (a) Single-stage classification model 1 (SSCM1), (b) single-stage classification model 2 (SSCM2). Part (a) shows a system processing fast features while part (b) shows a system processing all features.

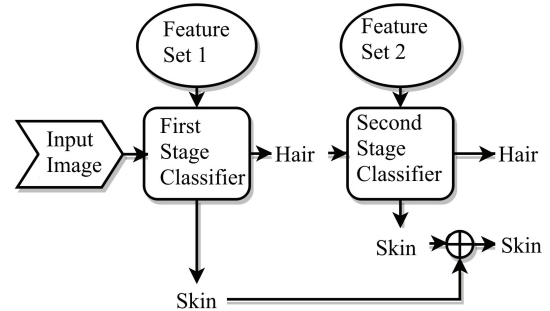


Figure 6. Two-stage classification model (TSCM). Faster first stage eliminates a large portion of nonhair regions providing a smaller dataset to be processed by the more accurate second stage.

5.2. Computation time

In order to make the fast/slow distinction between features, a threshold level is being determined with respect to the average processing times of each feature. Average processing times are calculated by using test patterns with predetermined size of 15×15 pixels. A 0.1 ms average processing time is chosen to be an appropriate threshold level for fast/slow feature distinction. Fastest calculated features are intensity mean-minimum intensity difference and intensity span. Slowest calculated feature is local minimum filter difference. With this threshold level, Features 1–6 are regarded as fast features while Features 7–12 are regarded as slow features.

5.3. Classification methods

In this study, LDA, SVM with linear kernel, DT, NB, and k-NN classification techniques [15] are evaluated in terms of speed and classification success rates. In order to calculate sensitivity, specificity and error rate of each classifier, 5-fold cross validation has been used by averaging the results of 500 independent repetitions. We use 5-fold cross validation such that the effect of grouping data into test and training is minimized. These criteria are calculated to evaluate test results quantitatively using all of the 12 features together with the classification techniques given above. Sensitivity, specificity, and error rate values for each of the classification technique are shown in Table 1. For k-NN classification technique, 5 nearest neighbors have been used which has shown the best performance with respect to other neighborhood numbers.

Table 1. Results for different classification techniques. Table shows several performance criteria including error rate, sensitivity and specificity. SVM yields the highest specificity while 5-NN yields the lowest error rate.

Class. tech.	Error rate	Sensitivity	Specificity
LDA	0.0167	0.9775	0.9890
NB	0.0274	0.9838	0.9613
Linear SVM	0.0142	0.9896	0.9818
DT	0.0289	0.9725	0.9695
5-NN	0.0124	0.9895	0.9856

As a result of cross validation tests, lowest error rate has been obtained by using 5-NN technique and the highest specificity value has been obtained by using SVM technique with linear kernel function. On the other hand, hair and skin pattern classification performance of NB and DT techniques are observed to be lowest compared to other methods.

In this study, another criterion to be taken into consideration is the average classification speed of each classification technique. In order to calculate the average classification time, each technique is trained with 169 hair and 169 skin patterns and tested with a hair and a skin pattern that is not included in the train set and the classification times for hair and skin patterns are averaged. This process repeated for 100 times with different tests and training sets, and the final results are averaged. NB is the fastest technique with 0.0006 s while other computation times are as follows: LDA 0.0011, SVM 0.0009, DT 0.0013, 5 NN 0.018 s. Highest performance for hair and skin classification have been obtained by using SVM and 5-NN techniques. In terms of classification speed SVM is two times faster than 5-NN technique. Consequently, SVM technique with linear kernel function is chosen to best classifier for this study. Highest performance for hair and skin classification have been obtained by using SVM and 5-NN techniques. In terms of classification speed SVM is two times faster than 5-NN technique. Consequently, SVM technique with linear kernel function is chosen to best classifier for this study.

5.4. Feature selection

Feature selection process is carried out for two different categories as described in Section 4.4. First, FS1 is selected by using only the fast feature set. Similarly, FS2 is selected by using all of the features (fast + slow features). 5-fold cross validation with SVM classification technique is utilized in order to compute the error rate of each feature set. Cross validation process is carried out for 100 random repetitions and the results are averaged. Selected feature sets with minimum error rate are features FS1= {2, 3, 4, 6} with an error rate of 0.012 and features FS2= {2, 5, 8, 10} with an error rate of 0.0099.

5.5. Cross validation

Both single-stage and two-stage classification models are evaluated with respect to the sensitivity, specificity and error rate criteria. 5-fold cross validation with 500 random repetitions is used in order to calculate these values. Analyzing the test results which are shown in Table 2 specificity value of the proposed TSCM is higher than both of the single-stage classification models. And with the help of biased classification in the first stage, sensitivity value of the TSCM does not fall below the sensitivity of SSCM1.

Table 2. Performance results for SSCM1, SSCM2, and TSCM. SSCM2 produces the lowest error rate.

Method	Error rate	Sensitivity	Specificity
SSCM1	0.0122	0.9891	0.9866
SSCM2	0.0101	0.9924	0,9874
TSCM	0.0107	0.9898	0,9886

5.6. Average processing times for single-stage and two-stage models

Classification time of the proposed TSCM is being considered as another evaluation criteria for the success of this model. Classification time of SSCM1, SSCM2, and TSCM are calculated by performing tests with 630×480 pixel skin images found in the image library. Average results are as follows: SSCM1 0.4236, SSCM2 1.0145, and TSCM 0.7215 s. Analyzing the test results which are shown in Table 2, it can be seen that the classification speed of SSCM1 is nearly two times faster than the classification speed of SSCM2. The main reason for this result is SSCM1 utilizes only fast features while SSCM2 uses more complex features as well. As it was expected the speed of the proposed TSCM is faster than the speed of SSCM2 while both of the models are utilizing the same complex features in the classification process. In summary, proposed TSCM can achieve a performance closer SSCM2 while it is faster.

5.7. Visual results

In order to evaluate the performance of the classification models visually, results for an example image are being shown in Figure 7 for SSCM1, SSCM2, and TSCM with the ground truth image.

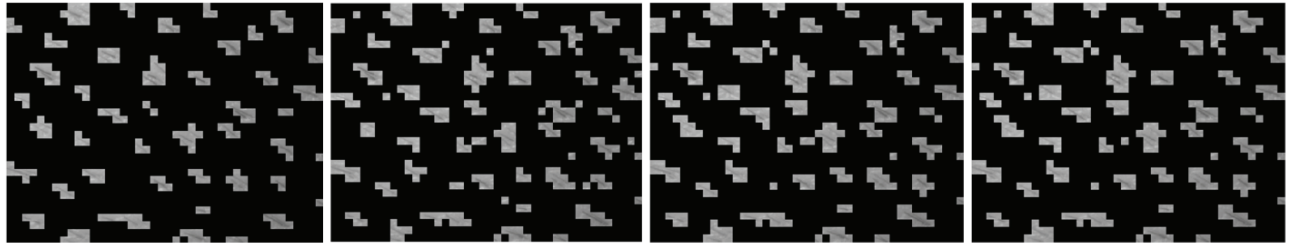


Figure 7. (a) Ground truth image, classification results obtained for (b) SSCM1, (c) SSCM2, (d) TSCM. Hair regions are cropped for easier visualization.

6. Conclusion

This study aimed to develop a real time hair region localization method such that purely hair regions are targeted during hair removal. In this way, we are able to avoid health risks caused by using the laser for the whole skin region. We proposed a feature-based hair region localization method by using image processing and

pattern recognition techniques, a first attempt in this area. Visual results shown in Figure 7 are also compatible with the quantitative results shown in Table 2. In this study, a two-stage hair and skin pattern classification technique is developed which is aimed to improve the performance of the single-stage classification model studied in our preliminary works [13]. The performance of the proposed two-stage classification model is compared to the single-stage classification models that are using first and second stage feature sets of the proposed model. Performance evaluation tests are carried out by comparing sensitivity-specificity values and the processing times of each classifier. As a result of the tests performed, it has been observed that the proposed TSCM is a good alternative compared to the single-stage models in terms of both speed and performance criteria. This work mainly focused on speeding up the small spot sized laser hair removal systems. Models are tested by using images taken from Mediterranean skin type who have dark hairs. Even though, laser hair removal is not very successful with light colored and white hair type, in the future studies, we plan to improve our train and test datasets with these hair types.

References

- [1] Dierickx CC, Grossman MC, Farinelli WA, Anderson RR. Permanent hair removal by normal-mode ruby laser. *Archives of Dermatology* 1998; 134 (7): 837-842. doi: 10.1001/archderm.134.7.837
- [2] Williams RM, Mary B, Christian M, Moy RL. Hair removal using the long-pulsed ruby laser. *Dermatologic Clinics* 1999; 17 (2): 367-372. doi: 10.1111/j.1524-4725.1998.tb04260.x
- [3] Grossman MC, Dierickx C, Farinelli W, Flotte T, Anderson RR. Damage to hair follicles by normal-mode ruby laser pulses. *Journal of the American Academy of Dermatology* 1996; 35 (6): 889-894. doi: 10.1016/s0190-9622(96)90111-5
- [4] Nahm WK, Tsoukas MM, Falanga V, Carson PA, Sami N et al. Preliminary study of fine changes in the duration of dynamic cooling during 755-nm laser hair removal on pain and epidermal damage in patients with skin types III-V. *Lasers in Surgery and Medicine* 2002; 31 (4): 247-251. doi: 10.1002/lsm.10104
- [5] Liewa SH, Ceriob R, Sarathchandrac P, Grobbelaara AO, Gaulta DT et al. Ruby laser-assisted hair removal: an ultrastructural evaluation of cutaneous damage. *British Journal of Plastic Surgery* 1999; 52 (8): 636-643. doi: 10.1054/bjps.1999.3195
- [6] Anderson RR, Parrish JA. Selective photothermolysis: precise microsurgery by selective absorption of pulsed radiation. *Science* 1983; 220 (4596): 524-527. doi: 10.1126/science.6836297
- [7] Lanigan SW. Incidence of side effects after laser hair removal. *Journal of the American Academy of Dermatology* 2003; 49 (5): 882-886. doi: 10.1016/S0190-9622(03)02106-6
- [8] Abbas Q, Celebi ME, Garcia IF. Hair removal methods: a comparative study for dermoscopy images. *Biomedical Signal Processing and Control* 2011; 6 (4): 395-404. doi: 10.1016/j.bspc.2011.01.003
- [9] Abbas Q, Garcia IF, Celebi ME, Ahmad W. A feature-preserving hair removal algorithm for dermoscopy images. *Skin Research and Technology* 2013; 19 (1): e27-e36. doi: 10.1111/j.1600-0846.2011.00603.x
- [10] Lee T, Ng V, Gallagher R, Coldman A, McLean D. Dullrazor: a software approach to hair removal from images. *Computers in Biology and Medicine* 1997; 27 (6): 533-543. doi: 10.1016/s0010-4825(97)00020-6
- [11] Fiorese M, Peserico E, Silletti A. VirtualShave: automated hair removal from digital dermatoscopic images. In: *IEEE International Conference of the Engineering in Medicine and Biology Society EMBC*; Boston, MA, USA; 2011. pp. 5145-5148. doi: 10.1109/IEMBS.2011.6091274
- [12] Nguyen NH, Lee TK, Atkins MS. Segmentation of light and dark hair in dermoscopic images: a hybrid approach using a universal kernel. In: *SPIE-The International Society for Optical Engineering*; San Diego, CA, USA; 2010. doi: 10.1117/12.844572

- [13] Avşar M, Yetik IS. Hair region localization with optical imaging for guided laser hair removal. In: Proceedings of IEEE 12th International Symposium on Biomedical Imaging ISBI; Beijing, China; 2014. pp. 1411-1414. doi: 10.1109/ISBI.2015.7164140
- [14] Vincent L. Morphological grayscale reconstruction in image analysis: applications and efficient algorithms. IEEE Transactions on Image Processing 1993; 2 (2): 176-201. doi: 10.1109/83.217222
- [15] Theodoridis S, Koutroumbas K. Pattern Recognition. 4th ed. New York, NY, USA: Academic Press, 2009.